

# Noise Reduction Using Multi-resolution Edge Analysis

Bo Jiang, Zia-ur Rahman  
Old Dominion University, Norfolk, VA 23529

## ABSTRACT

In this paper, a new noise reduction algorithm is proposed. In general, an edge—high frequency information in an image—would be filtered or suppressed after image smoothing. The noise would be attenuated, but the image would lose its sharp information. This defect makes the post-processing harder. One new algorithm performs connectivity analysis on edge-data to make sure that only isolated edge information that represents noise gets filtered out, hence preserving the overall edge structure of the original image. The steps of new algorithm are as follows. First, find the edge from the noisy image by multi-resolution analysis. Second, use connectivity analysis to direct a mean filter to suppress the noise while preserving the edge information. In the first step, we propose a new algorithm to find edges in a very noisy image. The algorithm is based on the analysis of a group of multi-resolution images obtained by processing the original noisy image by different Gaussian filters. After applied to a sequence of images of the same scene but with different signal-noise-ratio (SNR), this method is robust to remove noise and keep the edge. Also, through statistic analysis, there exists the regularity that the parameters of the algorithm would be constant with varying images under the same SNR.

**Keywords:** Noise Reduction, Edge Detection, Multi-resolution, Gaussian Filters, Connectivity Analysis

## 1. INTRODUCTION

Reducing the impact of noise on digital images has been an active topic of research through the years. Generally, the techniques for noise reduction have been based on mathematical analysis of the systems used to generate digital images, e.g., scanners and digital cameras. Based on this, system analysis allows one to develop image restoration filters<sup>1,2</sup> that analyze the different sources of noise and reduce their effect. Other researchers found some simple but effective method such as the mean, or smoothing, filter (MF) and the median filter<sup>3</sup> to be effective. While these techniques are quite useful, they have significant shortcomings in the presence of a high level of noise. Several researchers have shown the importance of using edge primitives as a basis for recognition in visual perception.<sup>4,5</sup> This edge pattern analysis can be used for both automatic assessment of spatially variable noise and as a foundation for new noise reduction methods.<sup>6</sup>

Recently, the trend in edge-detection is moving away from using neighborhood pixel differences to the estimate of local derivatives for detecting intensity changes. More attention is being paid to edge feature analysis, and, based on this, in trying to design new and effective noise reduction methods. Edges can be divided into basic categories,<sup>7,8</sup> such as ramp, step, stair, and pulse: different types have different shapes. These edges can be filtered with a Gaussian to estimate their slope.<sup>9,10</sup> Because noise can generally be assumed to be independent of signal, have little regional connectivity, and have random orientation, its estimate would be small under a Gaussian filter. Furthermore, it has been shown that the Gaussian is close to the optimal operator for different edges.<sup>11</sup>

In this paper, a new noise suppression algorithm is introduced. The most common way of noise reduction is to apply a low-pass filter to the noisy image. In general, this results in blurring or suppressing the edge features—high frequency information—in the image. Thus, while the noise is attenuated, the image loses sharpness and, hence, contrast. This trade-off between noise reduction and sharpness retention makes the use of the image for post-processing tasks considerably harder. To compensate for this drawback Kao and Chen,<sup>12</sup>

---

Contact: Bo Jiang (bjian001@odu.edu) is a PhD student at the Computational Intelligence and Machine Vision Laboratory at Old Dominion University. Zia-ur Rahman (zrahman@odu.edu) is an Associate Professor at ODU. He is affiliated with the Electrical and Computer Engineering Department and the Virginia Modeling, Analysis and Simulation Center (VMASC).

for example, have added an edge preserving stage in the processing approach. We have based our approach upon the algorithm presented by Rahman et al.<sup>13</sup> The premise of their approach to noise reduction is that the edges in the image should be preserved, and connectivity analysis can be used to classify edge or noise. They replace the pixels classified as “noise” by an average of their neighbors, hence reducing the the impact of noise at that location. Our new algorithm performs connectivity analysis on edge-data to make sure that only isolated edge information that represents noise gets filtered out, hence preserving the overall edge structure of the original image. The steps of new algorithm are as follows.

1. Find edges in the noisy image by multi-resolution analysis.
2. Use connectivity analysis to direct a MF to suppress the noise while preserving the edge information.

In the design of the algorithm, we carefully took into account a well-balanced compromise between noise reduction and feature preservation. The experimental results show that the proposed algorithm can improve the quality of removing noise on the images corrupted by Gaussian noise even for very low SNR values.

The organization of the rest of the paper is as follows. The details of the new algorithm are given in section 2. Experimental results and analysis are shown in section 3. In section 4, the conclusions are presented.

## 2. ALGORITHM

Steps 1–3 that follow describe the edge-detection algorithm that has been adapted from Beltran et al.,<sup>9</sup> and step 4 describes the connectivity analysis that is used to perform edge-preserving noise reduction.

1. Generate the multi-scale image representations:

$$G_j(m, n) = G(m, n) * F_j(m, n), \quad j = 1, \dots, 6 \quad (1)$$

$$F_j(m, n) = \exp\left(-\frac{m^2 + n^2}{\sigma_j^2}\right), \quad \sigma_j = 2^j \sigma_1, \quad j = 2, \dots, 6, \quad (2)$$

where  $\sigma_1$  is the standard deviation of  $F_1(m, n)$ , and can be varied depending upon the image under consideration.

2. Each image  $G_j, j = 1, \dots, 6$  has associated modulus  $M_j$  and phase  $P_j$  images.  $M_j$  and  $P_j$  are computed as:

$$DG_j^x = G_j D_x, \quad D_x = \begin{bmatrix} -1 & 1 \end{bmatrix} \quad (3)$$

$$DG_j^y = G_j D_y, \quad D_y = \begin{bmatrix} -1 & 1 \end{bmatrix}^T \quad (4)$$

$$M_j = \sqrt{(DG_j^x)^2 + (DG_j^y)^2} \quad (5)$$

$$P_j = \tan^{-1} \left[ \frac{DG_j^y}{DG_j^x} \right], \quad (6)$$

where  $[\ ]^T$  indicates vector transposition.

3. The  $M_j$  and  $P_j$  images are used to obtain the edge using a top-down search algorithm. For a pixel to be classified as an edge, it must satisfy the following two conditions:

$$M_j(m, n) > \tau_m, \quad \text{AND} \quad (7)$$

$$P_j(m, n) \approx \Phi(m, n), \quad j = 1, \dots, 6. \quad (8)$$

where  $\tau_m$  is a magnitude threshold value, and  $\Phi(m, n) = P_1(m, n)$ . Equation 8 can be rewritten as  $|P_j(m, n) - \Phi(m, n)| < \tau_p, j = 2, \dots, 6$ , where  $\tau_p$  is a small threshold value to take into account the

discrete nature of the computation of the phase,  $P_j$ . If both conditions are satisfied, then pixel at  $(m, n)$  in the noisy image would be judged to lie on an edge. Once the edge-pixel locations have been found, the connectivity analysis is used to denoise the original image.

Using images from all 6 scales typically results in very thick edges because of the heavy blurring associated with large values of  $j$  in Equation 2. Experimental results led to the employment of a 3-of-6 rule in which we use a combination of 3 out of the 6 possible scales to generate the output image. Different results can be obtained depending upon which scales are used. Small scales give finer edges but are more prone to letting noise through. Larger scales eliminate the noise but produce thick edges. Once the three optimal scales have been determined, a second variation results in producing better edge results. In this variation, we accept a pixel to be an edge pixel if there is a large value at that location in 2-of-3 scales. The orientation requirement is as before. This leads to more connected edges, but also allows more noise pixels to be classified as edges. We also found through experiments that parameters, such as  $\sigma_1$ ,  $\tau_m$ , and  $\tau_p$  can be kept constant for different images with the same signal-noise-ratio (SNR). However, these values should be adjusted as a function of the SNR.

4. For each non-zero pixel in the edge image we perform connectivity analysis, i.e., check if there is another edge in the edge image in a  $3 \times 3$  neighborhood centered at that pixel. If there is another edge, the non-zero pixel will be considered a signal edge, otherwise it would be considered as noise and eliminated. This is similar to the analysis used for hysteresis thresholding in the Canny edge operator.<sup>11</sup> Pixels that are classified as noise are used to replace the pixel in the original image by the output of a  $3 \times 3$  MF.

We compare the performance of the multi-resolution edge algorithm with three other edge segmentation operators: (i) Sobel,<sup>3</sup> (ii)  $3 \times 3$  smallest difference-of-Gaussian, or, lateral-inhibition (LIH),<sup>14,15</sup> and (iii) Canny.<sup>11</sup> In each case, we perform connectivity analysis after edge detection to denoise the original image. We discuss each of these algorithms in some detail in the following subsections. Their performance is shown in the next section.

## 2.1. Sobel Operator

The Sobel operator is one of the most popular edge detection operators. In its simplest form, it consists of two convolution kernels: one,  $S_H$  is designed to detect primarily horizontal edges, and the other,  $S_V$ , primarily vertical edges.

$$S_x = \begin{bmatrix} -1 & -2 & -1 \\ 0 & 0 & 0 \\ 1 & 2 & 1 \end{bmatrix} \quad S_y = \begin{bmatrix} -1 & 0 & 1 \\ -2 & 0 & 2 \\ -1 & 0 & 1 \end{bmatrix} \quad (9)$$

The edge pixel,  $e_s(m, n)$ , is then given by

$$e_s(m, n) = |G(m, n) * S_x| + |G(m, n) * S_y| \quad (10)$$

where  $G(m, n)$  are the pixels from the input image,  $G$ .

## 2.2. Lateral Inhibition

The smallest difference-of-Gaussian (DOG), or the lateral inhibition (LIH), operator drives its origin from the natural vision literature. The lateral inhibition terminology comes from its physical renditions, where a positive center pixel in a  $3 \times 3$  neighborhood is inhibited by all of its neighbors to produce a high pass signal. Mathematically, the output of the LIH is given by:

$$e_l(m, n) = G(m, n) * L \quad (11)$$

where  $e_l(m, n)$  is the edge output, and

$$L = \begin{bmatrix} -0.0675 & -0.1820 & -0.0675 \\ -0.1820 & 1.0000 & -0.1820 \\ -0.0675 & -0.1820 & -0.0675 \end{bmatrix}. \quad (12)$$

### 2.3. Canny Operator

The Canny operator is proposed by finding the optimization algorithm based upon three basic performance criteria: good SNR, good detection and localization, and only one response to a single edge. It is implemented as the following four steps:

1. Smoothing the image using Gaussian filtering.
2. Calculating the gradient magnitude and direction by using first order finite differences.
3. Imposing non-maximum suppression on the gradient value.
4. Detecting and connecting the edges by using hysteresis thresholding.

### 3. RESULTS

We have tested our method on color and grayscale images with SNRs varying from 1 to 10. The images used in the experiments were computer generated so the baseline images were noise free. This allowed us to add white Gaussian noise of varying amplitude to the data to generate images with a given mean-square SNR. The reason why we use these images is because the experimental results of the noise-reduction procedure can be compared with the original image to get a reasonable metric of performance. Of course, in real-life situations, we only have access to the noisy data so we cannot use fidelity analysis or other similar metrics to measure the performance of our algorithm.

Figure 1 shows an original, noise-free, image  $G$  and three noisy images,  $G_n$ , with different SNR values. In general, except when the  $\text{SNR} \approx 1$ , traditional edge detection methods can be used to find the edges that have been impacted by noise. Figure 2 shows  $G_j$  for the original noise free image,  $G$ , and Figure 3 shows the scaled images for  $G_{n1}$ . The  $F_j$  used for these image were generated using  $\sigma_1 = 2$ . This value of  $\sigma_1$  was deemed to be optimal after conducting a series of experiments. As can be seen from Figures 2 and 3, while noise suppression is small for  $j = 1, 2, 3$ ,  $|G_j - G_{n1j}|, j = 4, 5, 6$  is relatively small.

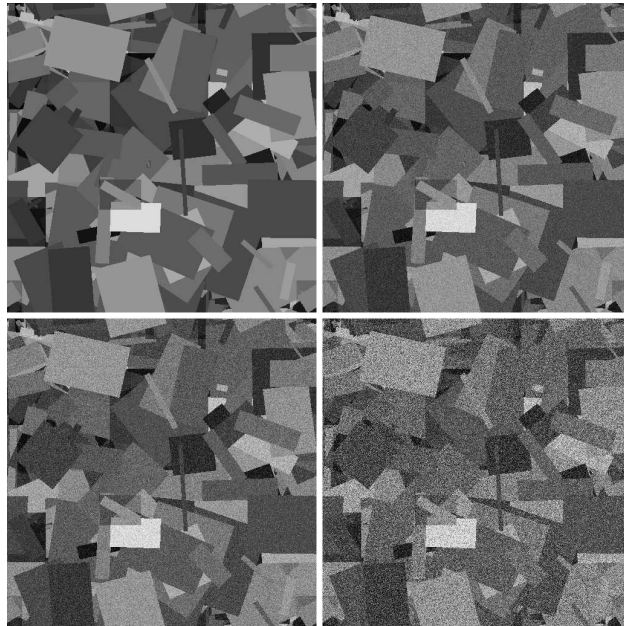


**Figure 1.** (top-left) Original image,  $G$ ; (top-right) noisy image  $G_{n10}$ ,  $\text{SNR} = 10$ ; (bottom-left) noisy image,  $G_{n5}$   $\text{SNR} = 5$ ; (bottom-right) noisy image,  $G_{n1}$ ,  $\text{SNR} = 1$ .

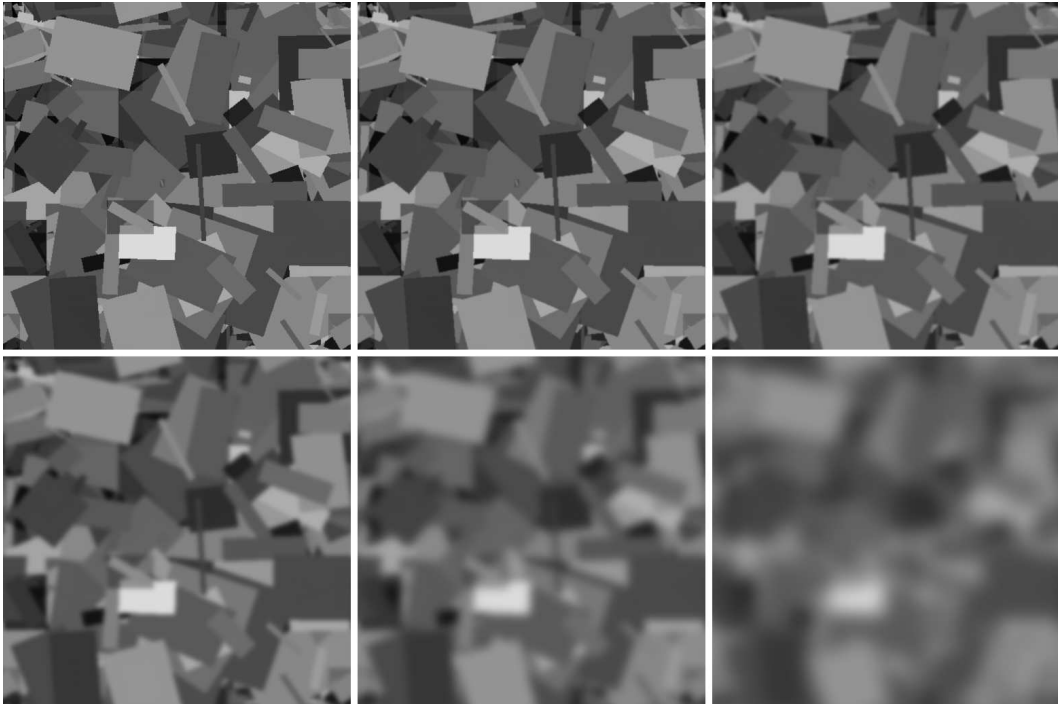


Figure 2: Scaled images for  $G$ .

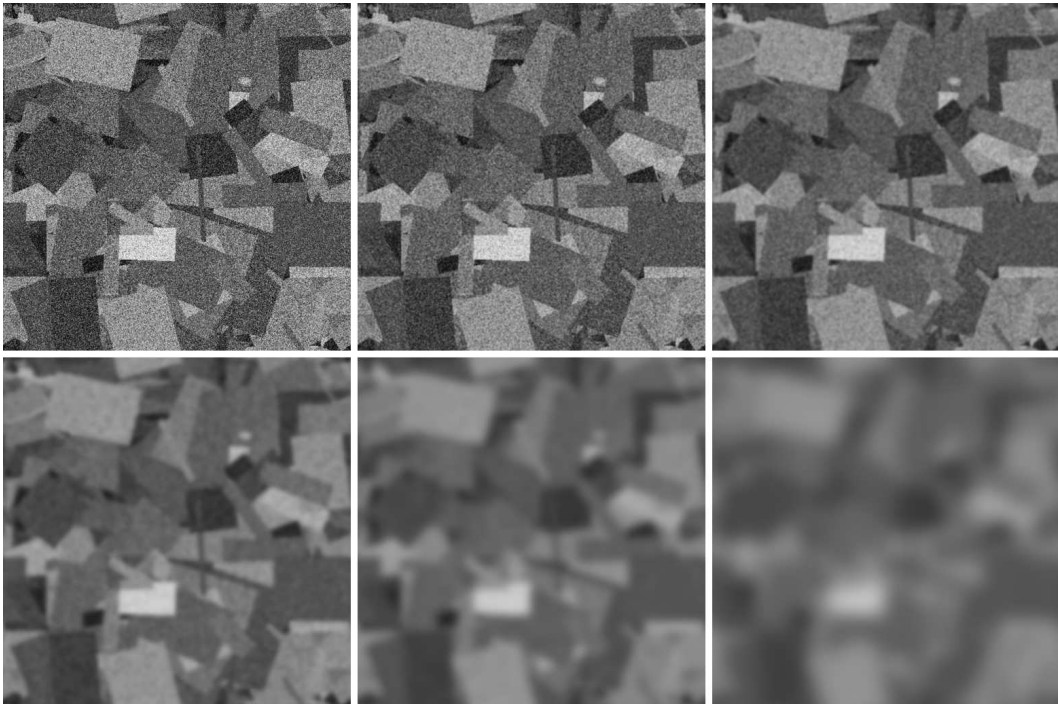
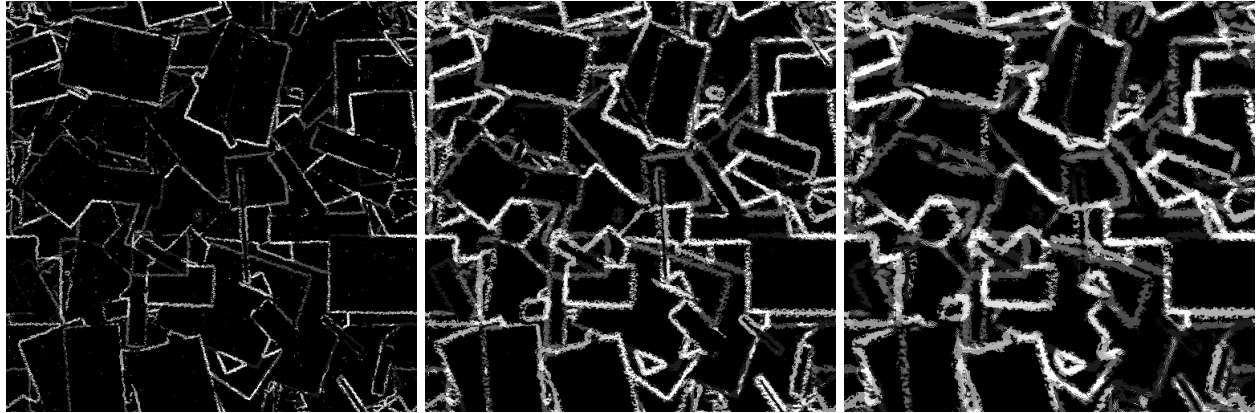


Figure 3: Scaled images for  $G_{n1}$ .

From our experiments we determined that it is not necessary to use all six scaled images to obtain an edge image: in general, three scales are enough. The question, then, is: which three scales should be used? From Figure 3, we see that smaller  $\sigma_j$  keep the image sharp and noisy, and vice visa. Just using the smallest or largest  $\sigma_j$  does not provide good performance. Larger  $\sigma_1$ , such as the one shown in Figure 3 (bottom-right) lose almost all the high frequency information and hardly gives any help for edge detection, a result confirmed by experiment. In Figure 4, different combinations of scales are shown. In each case, three neighboring scaled images were selected. We found that different combinations of scales required different values for  $\tau_m$  and  $\tau_p$ . While we had to relax the requirement on  $\tau_p$ , its impact on edge detection was not critical. However, varying  $\tau_m$  has a significant impact on the performance of the algorithm. Increasing  $\tau_m$  removes more noise, but also loses more edges.



**Figure 4.** The results of combination all 3 different layers. (left) 1, 2 and 3 layers, (center) 2, 3 and 4 layers, (right) 3, 4 and 5 layers.

Using the same  $\sigma_1$ , another new scheme was introduced. A pixel at  $(m, n)$  was considered to be an edge pixel if  $M_j(m, n) > \tau_m$  for 2-of-3 scales, rather than for 3-of-3 scales as shown in Figure 4. Results for this scheme are shown in Figure 5. While this new scheme leads to more connected edges, it also allows more noise pixels to be classified as edges. However, the visual impact is better than the 3-of-3 scheme because the edges are finer. The value for  $\tau_m$  changes slightly for optimal results, but  $\tau_p$  is the same as that used in Figure 4.

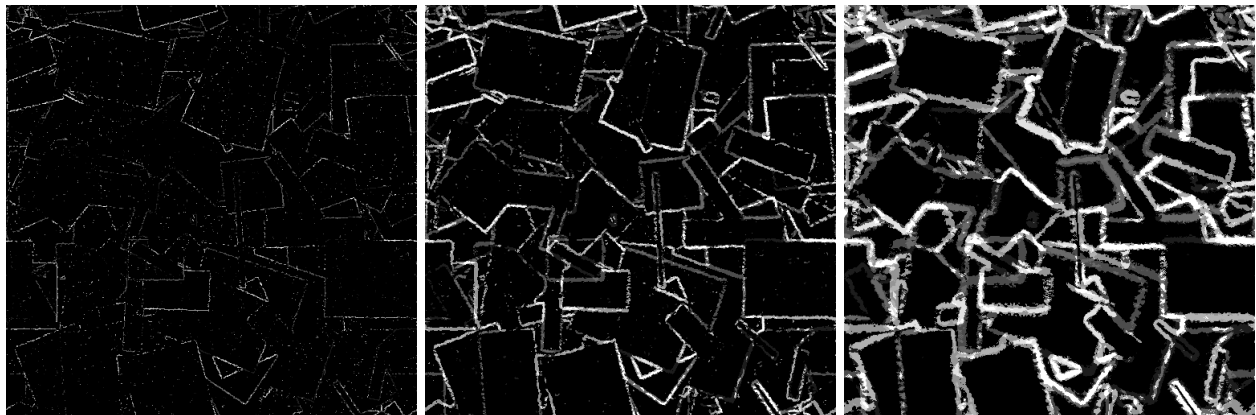


**Figure 5.** The results of combination 2 out of 3 different layers. (left) 1, 2 and 3 layers, (center) 2, 3 and 4 layers, (right) 3, 4 and 5 layers.

For the 3-of-3 and 2-of-3 operators, using different Gaussian filters to suppress the noise would make the edges thicker as  $\sigma_1$  increases. Thinner edges can be produced only at the cost of classifying more noise pixels as edge pixels, especially for very low SNRs. We have determined experimentally that if SNR is  $> 10$  higher, then the proposed algorithms can produce edges that are as thin as those produced by traditional algorithms for the noise-free case.

In order to evaluate the performance of proposed algorithm, we compare its performance with the traditional methods described in Sections 2.1–2.3. The results are shown in Figure 6. Both 3-of-3, and 2-of-3 methods produce similar results, though 2-of-3 classifies more pixels as edges, and is, hence, noisier. But, based on connectivity analysis used to differentiate noise or edges, a little more noise and edges would be better for the next processing step. The Sobel operator is badly affected by noise, as all noise causes an edge transition. LIH seems to lose connectivity since it is primarily a point detector. The Canny operator is good at suppressing noise and detecting edges because it uses a Gaussian filter to smooth the image first. However, the Canny operator is very sensitive to the two thresholds used for hysteresis thresholding. This sensitivity results in a number of small curves or projections for very low SNRs. This impacts the denoising element of our proposed algorithm.

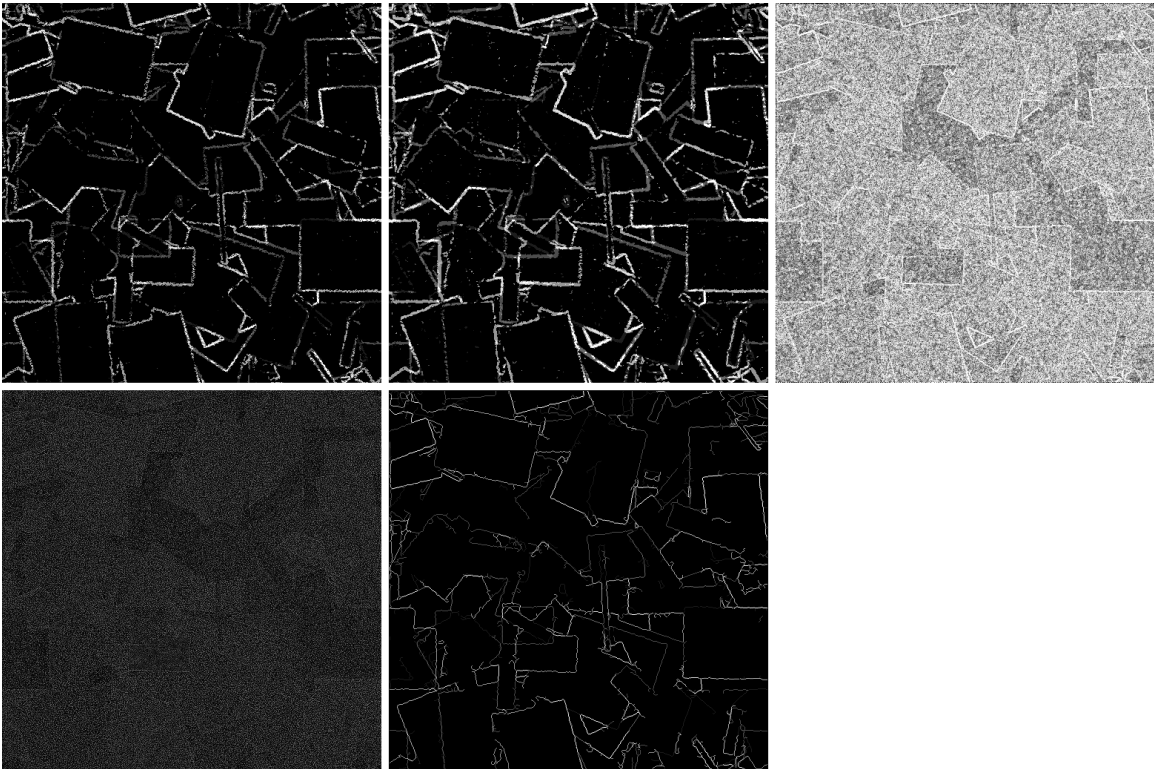


**Figure 6:** (top-left) 3-of-3, (top-center) 2-of-3, (top-right) Sobel, (bottom-left) LIH, (bottom-right) Canny.

Figure 7 shows the edge images obtained with the methods used to generate Figure 6, but for the noise-free case. In the noise-free image, all the methods get excellent results, with few differences in performance. Both 3-of-3 and 2-of-3 methods give similar results, but the edges for the 3-of-3 method are finer than those produced by the 2-of-3 method. This is because fewer pixels are eliminated using Equation 8 for the 2-of-3 methods since the comparison take place over fewer scales. Both methods produce edges that are thicker than those produced by other algorithms. The Sobel operator correctly finds the edges in the image. However, the edges it produces are thicker than those produced by the LIH and Canny operators. LIH marks the location of the edges precisely and the edges are thin. Canny operator also performs well and produces thin edges.

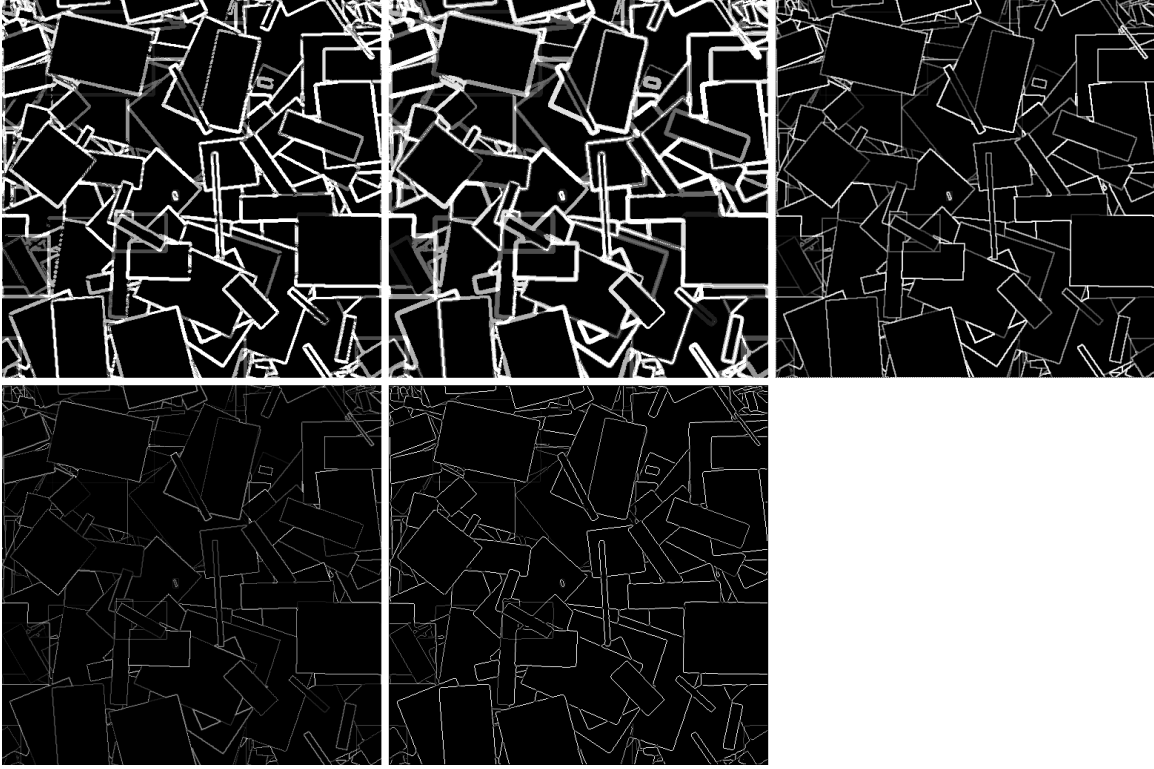


**Figure 7:** (top-left) 3-of-3, (top-center) 2-of-3, (top-right) Sobel, (bottom-left) LIH, (bottom-right) Canny.

So far we have evaluated the impact of varying the number of scales and the parameters  $\sigma_1$ ,  $\tau_m$  and  $\tau_p$  on the performance of the edge-detection algorithm. Recall, that the overall denoising process relies on the edge-detection mechanism followed by noise suppression at those locations where edge pixels do not exist. We also introduced the idea of edge connectivity analysis to determine which edge pixels were actually produced due to noise. In order to determine the effectiveness of this approach, we performed two tests. In the first case, we applied a blurring filter to every pixel that was not an edge pixel without performing edge connectivity analysis to determine if it were a noise pixel or not. In the second case, we performed edge analysis and further reduced the total number of edge pixels by those that were classified as noise. Figure 8 shows the output of the full noise-reduction mechanism and also, as a final comparison, the noise-reduction achieved by applying just the mean filter (MF). Experiments show that using edge analysis eliminates noise along the boundaries of regions with intensity transitions and produces an overall less noisy image. However, the impact on sharpness and contrast is minimal. The 3-of-3 and 2-of-3 methods are able to eliminate more noise than Sobel and LIH because of better edge detection and localization. The performance of the Canny operator is similar to that of the proposed method. The MF produces good results but the image is blurrier than the one produced by the other methods.

A commonly used metric of similarity between two images  $G_1$  and  $G_2$  is the *fidelity*,  $\mathcal{F}(G_\infty, G_\epsilon)$  defined as

$$\mathcal{F}(G_1, G_2) = 1 - \frac{\sum_{m=0}^{M-1} \sum_{n=0}^{N-1} (G_1(m, n) - G_2(m, n))^2}{\sum_{m=0}^{M-1} \sum_{n=0}^{N-1} G_1(m, n)^2}. \quad (13)$$

The fidelity metric corresponds fairly closely with visual judgment for comparing images. In order to measure

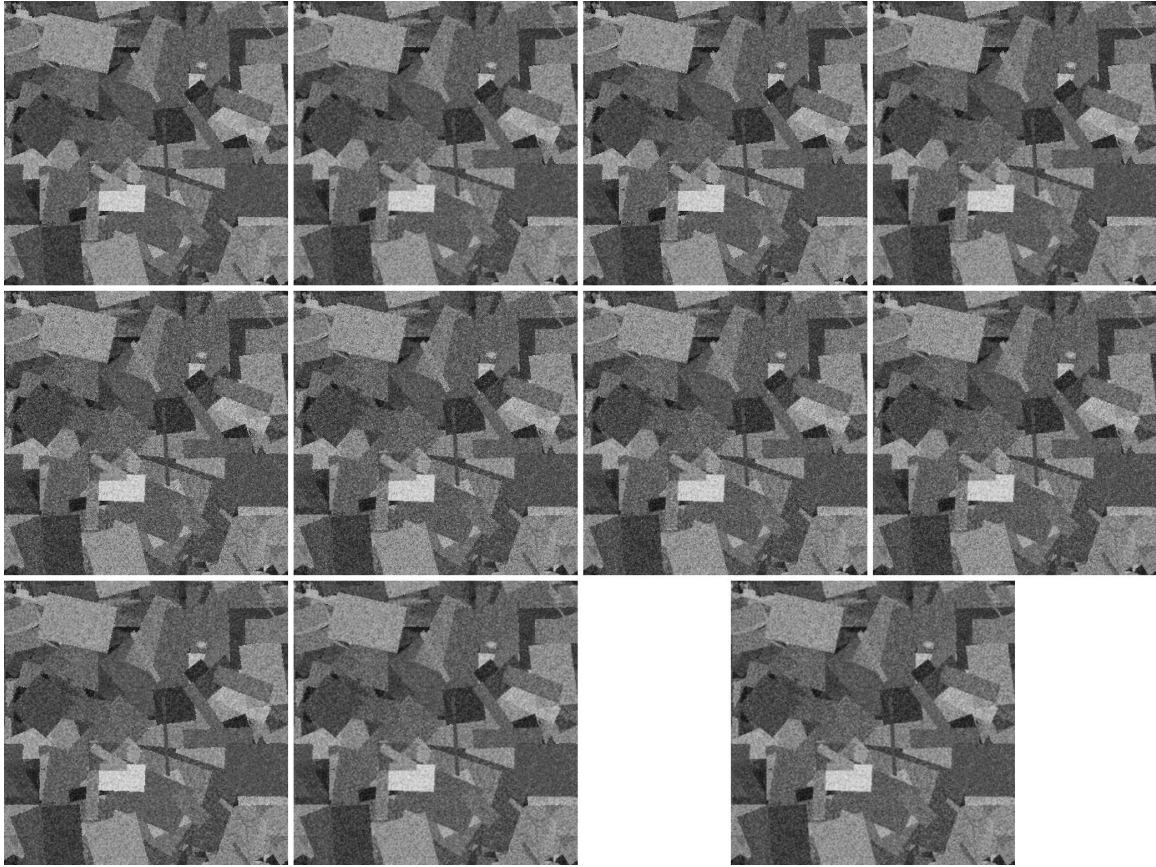


**Figure 8.** Figure 8. (top-row-left) 3-of-3 without edge analysis; (top-row-second) 3-of-3 with edge analysis; (top-row-third) 2-of-3 without edge analysis; (top-row-right) 2-of-3 with edge analysis; (second-row-left) Sobel without edge analysis; (second-row-second) Sobel with edge analysis; (second-row-third) LIH without edge analysis; (second-row-right) LIH with edge analysis; (bottom-row-left) Canny with edge analysis; (bottom-row-second) Canny without edge analysis; (bottom-row-right) MF.

the performance of our noise-reduction approach, we compute  $\mathcal{F}(G, G_p)$ , where  $G_p$  is variously produced by edge-directed noise reduction using the Sobel, LIH, Canny, and our two methods, and  $G$  is the original noise-free image. The results are tabulated in Table 1. Rahman et al<sup>13</sup> reported that the median filter achieved the best result. In this paper, we did not use the median filter, but we see that the MF performs as well as in terms of fidelity as the edge-directed noise reduction. We can explain this (slightly) unexpected result by the observation that fidelity is a gross measure of visual similarity so a blurred image compared with its original unblurred version would result in high fidelity, while visual comparison may not come to the same conclusion. The results show the proposed methods and Canny operator are effective in saving edges and removing noise. Table 1 also shows the effect of edge analysis. Under edge analysis, the fidelity results are better or the same as

Fidelity	Original Image	Noisy Image (SNR = 1)	Sobel	LIH	Canny	3-of-3	2-of-3	MF
Without edge analysis	1.00	0.78	0.91	0.93	0.96	0.96	0.95	0.96
With edge analysis	1.00	0.78	0.93	0.94	0.96	0.96	0.96	0.96

**Table 1:** Fidelity improvement with noise reduction

those without edge analysis.

As we had stated in the beginning of this paper, we had found that the value of the parameters needed to be changed depending upon the value of the SNR. From observation we see that to find thinner edge  $\sigma_1$  should be decreased, and the  $\tau_m$  should be increased otherwise more edges and more noise would be gotten. At the same time, due to small  $\sigma_1$ , the residual noise would be higher and affect the edges, making it harder to differentiate the edges and noise. Under these conditions, though the edge might be thinner, the noise would be worse not just crowded around the true edges but also spread in non-edge areas. However, since we do not use all the scales, reducing  $\sigma_1$  means that we may use a different set of scales that correspond to the same  $\sigma_j$  values. So the overall impact of changing  $\sigma_1$  is in selecting different scale rather than changing overall performance. However, the same cannot be said about  $\tau_m$ . Figure 9 shows the impact increasing SNR on the threshold value. As SNR increases,  $\tau_m$  decreases. This make intuitive sense since less noise in the image (higher SNR) corresponds to fewer false edges in the image corresponding to noise and hence does not require a larger threshold to eliminate such edges.

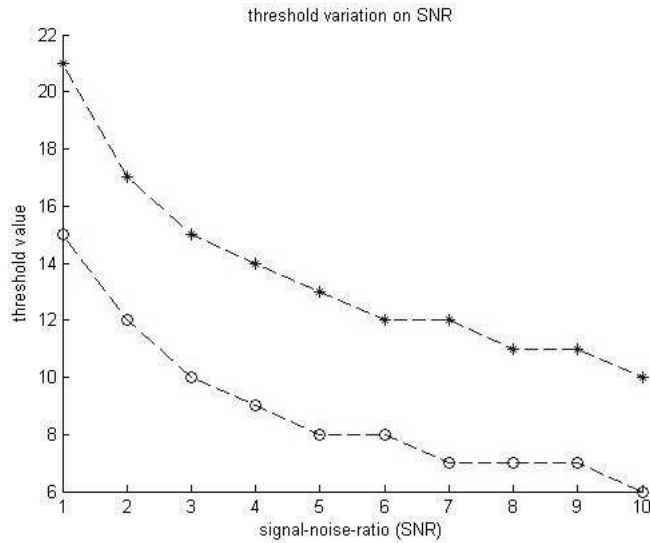


**Figure 9:** Threshold variation based on different SNR: \* stands for the color image, and o means the grayscale image.

#### 4. CONCLUSION

In this paper we proposed an algorithm based on multi-resolution processing and edge analysis to help preserve edge information during noise suppression. A group of Gaussian filters, proven to be close the optimal edge operator, was used to generate the multi-resolution images from the noisy image. Based on analysis of those different scaled images, pixels corresponding to true edges and noise can be obtained. After that, the edge image is used to direct noise suppression using the MF. Connectivity analysis is used to further differentiate edge pixels that are due to signal and those that are due to noise. Finally, the noise-reduced image is obtained. Experiments show that this new algorithm is effective even for very low SNR values.

#### ACKNOWLEDGMENTS

The authors wish to thank the NASA Aviation Safety Program, Intelligent Integrated Flight Deck, External Hazards for the funding which made this work possible.

## REFERENCES

1. C. L. Fales, F. O. Huck, and R. W. Samms, "Image system design for improved information capacity," *Applied Optics* **23**(6), pp. 872–888, 1984.
2. F. O. Huck, C. L. Fales, J. A. McCormick, and S. K. Park, "Image-gathering system design for information and fidelity," *Journal of the Optical Society of America A* **5**(3), pp. 285–299, 1988.
3. R. C. Gonzalez and R. E. Woods, *Digital Image Processing*, Addison-Wesley, Reading, MA, 1993.
4. D. J. Jobson, "Spatial vision processes: From the optical image to the symbolic structures of contour information," Tech. Rep. 2838, NASA, Washington, DC, November 1988. NASA Technical Paper.
5. D. Walters, "Selection of image primitives for general-purpose visual processing," *Computer Vision, Graphics, and Image Processing* **37**, pp. 261–298, February 1987.
6. D. J. Jobson, Z. Rahman, G. A. Woodell, and G. D. Hines, "The automatic assessment and reduction of noise using edge pattern analysis in nonlinear image enhancement," in *Visual Information Processing XIII*, Z. Rahman, R. A. Schowengerdt, and S. E. Reichenbach, eds., Proc. SPIE 5438, 2004.
7. D. J. Williams and M. Shah, "Edge characterization using normalized edge detector," *CVGIP: Graph. Models Image Process.* **55**(4), pp. 311–318, 1993.
8. J. R. Beltran, J. García-Lucía, and J. Navarro, "Edge detection and classification using Mallat's wavelet," in *Proceedings of the IEEE International Conference on Image Processing*, pp. 293–297, 1994.
9. J. Beltran, F. Beltran, and A. Estopanan, "Multiresolution edge detection and classification: noise characterization," in *Proceedings of the IEEE International Conference on Systems, Man, and Cybernetics*, pp. 4476–4481, 1998.
10. G. Palacios and J. Beltran, "Cell nuclei segmentation combining multiresolution analysis, clustering methods and colour spaces," in *Proceedings of the International Machine Vision and Image Processing Conference*, pp. 91–97, 2007.
11. J. Canny, "A computational approach to edge detection," *IEEE Transactions on Pattern Analysis and Machine Intelligence* **8**(6), pp. 679–698, 1986.
12. W. Kao and Y. Chen, "Multistage bilateral noise filtering and edge detection for color image enhancement," *IEEE Transactions on Consumer Electronics* **51**, pp. 1346–1351, November 2005.
13. Z. Rahman and D. J. Jobson, "Noise, edge extraction and visibility of features," in *Visual Information Processing XIV*, Z. Rahman, R. A. Schowengerdt, and S. E. Reichenbach, eds., Proc. SPIE 5817, 2005.
14. F. O. Huck, C. L. Fales, and Z. Rahman, *Visual Communication: An Information Theory Approach*, Kluwer Academic Publishers, Norwell, MA, 1997.
15. C. L. Fales, F. O. Huck, R. Alter-Gartenberg, and Z. Rahman, "Image gathering and digital restoration," *Philosophical Transactions of the Royal Society of London A* **354**, pp. 2249–2287, Oct. 1996.